J. Mol. Model. **1995**, *1*, 143 – 149

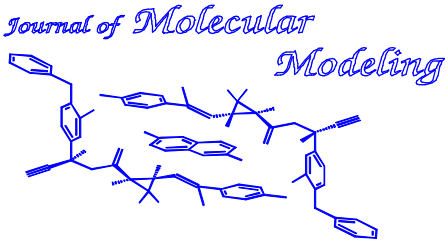

Study of the Interactions Between Neurophysin II and Dipeptide Ligand by Means of Molecular Dynamics

Rajmund Kazmierkiewicz, Cezary Czaplewski, Bernard Lammek, Jerzy Ciarkowski*

Faculty of Chemistry, University of Gdansk, Sobieskiego 18, PL-80-952 Gdansk, Poland

Bogdan Lesyng

Department of Biophysics, University of Warsaw, Zwirki i Wigury 93, PL-02-089 Warsaw, Poland

Received: 3 May 1995 / Accepted: 11 July 1995

Abstract

The nonapeptide hormones oxytocin (OT) and vasopressin (VP), while transported in the posterior pituitary, are packaged into neurosecretory granules (NSG) in the form of high associates with disulfide-rich proteins known as neurophysin I (NPI) and neurophysin II (NPII), respectively. In the NSG, neurophysins serve as carrier proteins to the hormones, until the latter are dissociated upon secretion into blood. To shed more light on molecular self-recognition between NPs, and between NPs and their ligands, we have studied their molecular association, using as a starting point the recently published solid-state structure (C^{α}-trace) of the neurophysin II-dipeptide complex. Another purpose of this work was the development of reliable strategies for molecular modeling, that would utilize minimal structural information (like C^{α} trace and/or structural homology) yet be useful for studies of protein/ligand interactions. An initial all-atom representation of the protein-peptide complex (2:2) was obtained by the conversion of the C^{α}-carbon trace deposited in the Brookhaven Protein Data Bank (file 1BN2), using the InsightII/Biopolymer modules from the suite of programs supplied by Biosym Technologies, San Diego. The free NPII homodimer was obtained by removal of the dipeptide ligands from the starting structures. Both associates, after initial immersion in water, were submitted to gradual (side chains first then all atoms) minimization of energy. Subsequently, they were thermally equilibrated and submitted to the molecular dynamics (AMBER 4.0) at 300K, until the total energy was stabilized. The structures, averaged over the last 20 ps of the dynamics, were compared with the starting C^{α}-trace and among themselves. The protein/ligand complex, simulated in water, compares favourably with the solid-state reference. An allosteric mechanism for the NPII dimer/ligand interaction is proposed and discussed.

Keywords: neurophysin/dipeptide complex, peptide ligand interactions, association, molecular dynamics

* *To whom correspondence should be addressed*

Introduction

The nonapeptide hormones oxytocin (CYIQNCPLG-NH_2, OT) and vasopressin (CYFQNCPRG-NH_2, VP) are synthesized in the hypothalamus as parts of common precursors with their associated carrier proteins neurophysin I, NPI, and neurophysin II, NPII, respectively [1]. The processing of the precursors into hormones complexed 1:1 with NPs occurs in the neurosecretory granules, NSG, of the posterior pituitary [2], where subsequently the NPs serve as carrier proteins to the hormones until the latter are dissociated upon secretion into blood. NPI and NPII are small disulfide-rich proteins of 93-95 amino acid residues, 7 disulphide bridges per molecule, very high sequence homology and almost identical hormone-binding and self-association properties [3]. It is believed that NPs, while carrying their hormones in the NSGs, are self-associated into dimers and/or higher oligomers [3,4].

Recently, the solid-state structure of NPII[1-86] in a complex with a dipeptide 4-I-Phe-Tyr-NH_2 was solved at 2.8 Å resolution by X-ray crystallography [5], Fig. 1. The three-dimensional structure, while confirming the formerly implied significance of the hormone's residues 1 and 2 in binding [3], provided details on the location, conformation and interaction of the ligand and the binding site of NPs. The protein/ligand complex has appeared to be associated into a dimer of dimers as the smallest asymmetric unit [5]. The four monomers have identical internal organization. In a monomer, all seven disulphides seem to be necessary to maintain the native three-dimensional architecture of the neurophysins. Their reduction, accompanied with denaturation, enables reconstruction only of a tiny fraction of the protein to the native state [6].

Our current interest is the *de novo* modeling of the protein-ligand interactions, using sequence homology and/or a low-resolution structure information. In this respect, the NPII/dipeptide complex presents an ideal testing model since its geometry, deposited in the Brookhaven Protein Data Bank [7] as a C^{α}-trace only, provides a low-resolution information appropriate for further refinement. On the other hand, the original work [5] unveils and discusses details of the peptide-ligand interaction at the atomic-resolution level (see ref. [5], Fig. 4), thus providing an excellent reference for a critical evaluation of the model building procedures employed.

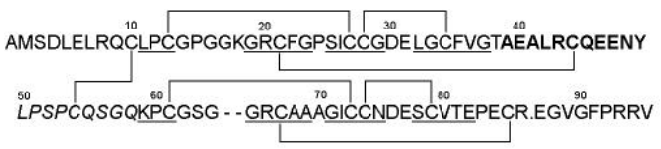

Figure 1a. *The sequence of bovine NPII. The ß-strands are underlined, the 3_{10} helix is printed in bold and the inter-domain connection in italic. The C-terminal fragment, not included in the X-ray study [5], is separated with a dot. The homological fragments in the two structurally similar domains are aligned vertically one under the other.*

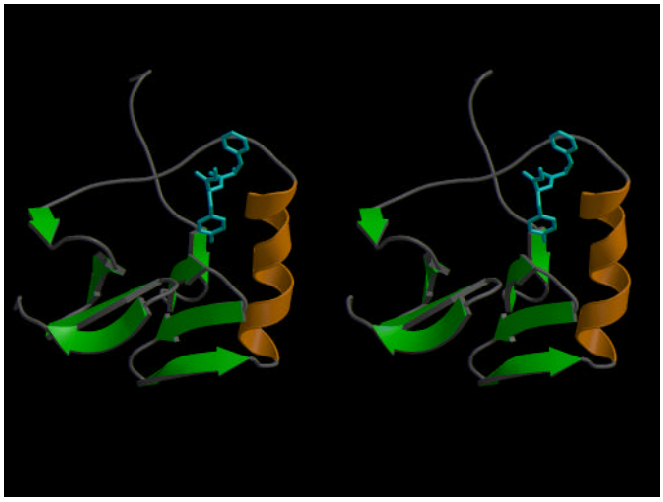

Figure 1b. *The structure (C^{α}-trace) of a NPII monomer with bound dipeptide [5]. The NPII molecule is made up of two highly homologic domains, composed of similar four-stranded antiparallel ß-sheets. In the first domain (blue), the ß-sheet is immediately followed by a 3_{10} helix, having no match in the second one (red). Both domains are connected by a relatively loose backbone fragment, supported by an* inter-*domain disulphide bridge Cys10-Cys54. The remaining 6 disulphide bridges crosslink the* intra-*domain architecture: the bridges 13-27, 21-44 and 28-34 in the first domain, and the bridges 61-73, 67-85 and 74-79 in the second one. The dipeptide ligand, represented with a bar, is seen in the binding loop (ENYLPSPC, 47-54) composed of the end of the 3_{10} helix (AEALRCQE<u>ENY</u>, 39-49) and the beginning of the inter-domain connection (<u>LPSPC</u>QSGQ, 50-58).*

Keeping in mind reliable strategies to molecular modeling as a requisite, another purpose of this work is to get more insight into the intrinsic stability of the NP molecule, as well as to shed more light on molecular self-recognition between NP monomers, and between NPs and their ligands. The specific model chosen in this work is the NPII/Phe-Tyr-$NHCH_3$ complex, which lacks 4-I on Phe1 and adds a carbon on the C-terminal amide, compared to the original ligand [5]. Neither of these changes impairs ligand's affinity [3,5]. On the other hand, the *C*-terminal *N*-methylation of the ligand introduces the C^{α}-carbon of the residue 3 of the ligand as a part of an extended template for future alignments at docking the hormones by simple replacements of the dipeptide in the NP binding sites.

The latter is pertinent to the third goal of this work, which is the development of a reliable starting template for subsequent inserting VP to NPII and OT to NPI binding sites, in order to carry out respective simulations with the hormones themselves as ligands. The hormone/NP interactions are currently being subject to similar investigations, to be published in a due time.

Methods

All computer-intensive calculations were done either on CRAY Y-MP/EL-98 in the Interdisciplinary Center for Mathematical and Computer Modeling at the University of Warsaw (ICM UW), or on SGI POWER CHALLENGE 4xR8000 in the Informatics Center of the Metropolitan Academic Network (IC MAN) in Gda´nsk. Interactive modeling, both in Warsaw and in Gda´nsk, was done using SGI INDY or INDYGO workstations. The images for presentation were prepared using the program CHEM-X [8].

For construction of the dimer bound with two dipeptide molecules, the units 1 and 2 of the tetramer, deposited as an "α-carbon trace" (file 1BN2) in the Brookhaven Protein Data Bank [7], were utilized. The α-carbon trace was converted into an initial all-atom representation using the INSIGHTII/BIOPOLYMER modules, implemented in BIOSYM's molecular modeling software [9] available at ICM UW. In order to remove large nonbonded repulsions between side chains, the initial $NPII_2$/$dipeptide_2$ complex thus prepared, was submitted to the minimization with the C^{α}-carbon atoms constrained, using the DISCOVER force field. In the next step, all disulphide bridges were locked. This was done by simultaneously constraining (firmly) the positions of all α-carbon atoms and (softly) the valence geometry, i.e. bonds and angles, within all the $C^{\alpha}C^{\beta}SSC^{\beta}C^{\alpha}$ units. With these constraints in effect, a minimization was done again using DISCOVER module. Subsequently, all side chains belonging to the window presented in Fig. 4 of Ref. [5] were manually so adjusted as to visually comply with the figure. The same thing was done with the ligand. The protein backbone fragments in the window did not need adjustments. All adjustments were simultaneously done in both monomers.

Since then on, all energy calculations were done using the program AMBER ver. 4.0. [10]. Subsequently, the C^{α}-constrained minimization was continued through 20000 cycles, using BELLY option of MINMD module in AMBER. In the next step, the $NPII_2$/$dipeptide_2$ complex was immersed (using EDIT routine in AMBER) into a rectangular box containing ca. 5600 TIP3P water molecules [11], which, together with the protein, made up some 18500 atoms. For a typical box size of 87.6 Å x 50.2 Å x 47.3 Å this would correspond to the concentration of ca $8.0 \cdot 10^{-3}$ mol·dm^{-3}. Minimum thickness of the solvent shell along the X, Y, and Z axes was 8 Å. The energy (AMBER) was then minimized with no constraints, using periodic boundary conditions. After 5000 cycles the minimization was switched over from the steepest descent to the conjugate gradient method. Maximum number of cycles in the minimization was 10000.

After energy was minimized, the system was thermally equilibrated. This consisted of a number of molecular dynamics, MD, with E(total) constant and velocities assigned from Maxwellian distribution, at temperatures 10 K, 100 K, 200 K, and 300 K, (10 runs 0.1 ps long per each temperature). Resampling of velocities from the Maxwell-Boltzmann distribution was applied during the equilibration to remove hot and/or cold spots (high/low levels of kinetic energy, localized in small areas). Having thermal equilibration completed, the system was submitted to 40 ps of MD proper at temperature 300 K, with the SHAKE option on, which enabled the time step of 1 or 2 fs. Both in the AMBER minimizations and dynamics, the residue-based cutoff was taken at 9 Å and the dielectric constant equal to 1.

The initial free NPII dimer ($NPII_2$) was obtained by removing the dipeptides from the initial $NPII_2$/$dipeptide_2$ complex. It was further processed as described above.

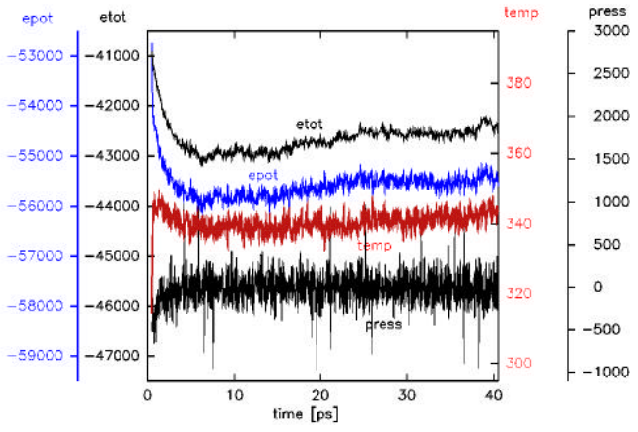

Figure 2. *The $NPII_2$/$dipeptide_2$ complex: Evolution of the total energy, the potential energy, the temperature and the pressure over the time range of 40 ps.*

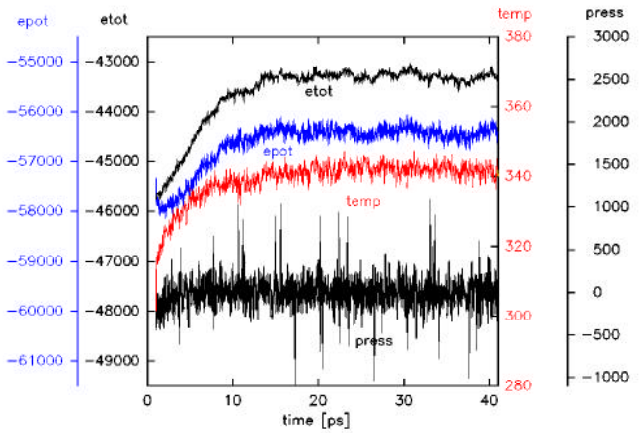

Figure 3. *The NPII dimer: Evolution of the total energy, the potential energy, the temperature and the pressure over the time range of 40 ps.*

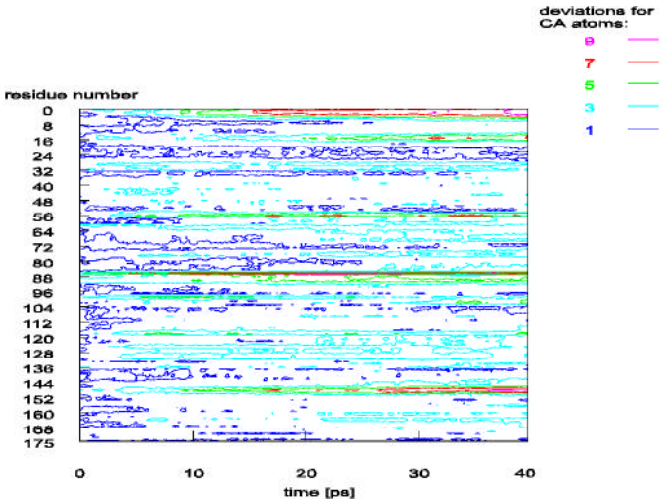

Figure 4. *The NPII$_2$/dipeptide$_2$ complex: Evolution of the geometry over the time range of 40 ps. The contour plot illustrates the fluctuations and/or drifts (in Å) of the C$^{\alpha}$ carbon atoms from their starting positions. The counting of the amino acid residues is contiguous over the four objects in the complex. Thus, the first NPII monomer (1-86) is immediately followed by the second one (87-172) which, in turn, is followed by the first (173-4) and the second (175-6) dipeptide. The deviations (if present) for residues 1-7, 84-86, 87-93 and 170-172 concern the* N- *and* C-*termini in either monomer and such should be disregarded. The remaining deviations are measure of the local "structural drifts" building up during the MD simulation. Thus, in the first monomer there are structural drifts around G16 (first domain first loop) and around S56 (interdomain connection), whereas in the second monomer there is a profound structure drift involving residues 146-150 on the plot (PCGSG, 60-64 corrected), corresponding to the first loop in the second domain.*

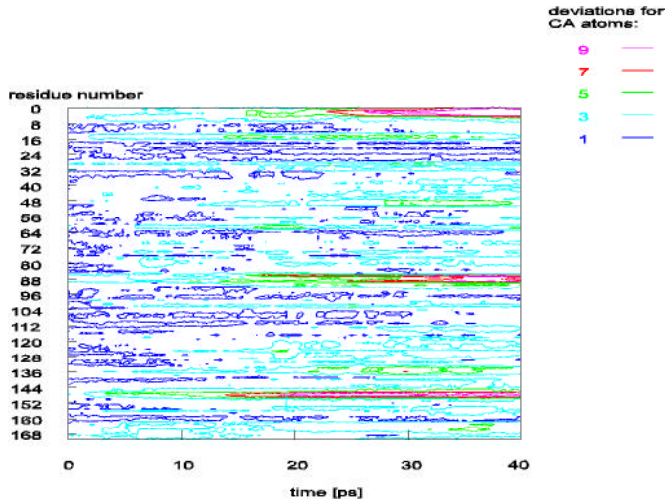

Figure 5. *The NPII dimer: Evolution of the geometry over the time range of 40 ps. The contour plot illustrates the fluctuations and/or drifts (in Å) of the C$^{\alpha}$ atoms from their starting positions. The counting of the amino acid residues is contiguous over both NPII monomers. Thus, the first NPII monomer (1-86) is immediately followed by the second one (87-172). The deviations (if present) for residues 1-7, 84-86, 87-93 and 170-172 concern the* N- *and* C-*termini in either monomer and such should be disregarded. The most significant structural drift is observed for residues 147-151 (CGSGG, 61-65 corrected), corresponding again to the first loop of the second domain in the second monomer, comp. Fig. 4, and less profound one around residue 138 (S52 corrected), corresponding to the apex of the binding loop.*

A typical 40 ps dynamics consumed 115 h of the CPU time on the CRAY (step 2 fs, the SHAKE option on) and 50 h of the CPU time on the SGI POWER CHALLENGE (step 1 fs, SHAKE on).

Results and discussion

The time evolution of energy for the NPII$_2$/dipeptide$_2$ (ligand associating) and the NPII$_2$ (free) dimer is shown in Figs. 2 and 3, respectively. It is clearly seen that the newly constructed NPII$_2$/dipeptide$_2$ complex needs nearly 10 ps of the dynamics, see Fig. 2, to achieve reasonably stabilized fluctuations in time. A dramatic drop in the total energy during this time period is associated with the accommodation and/or some penetration of water molecules by the protein's surface and/or through the protein's body. For a tightly packed system like the NPII$_2$/dipeptide$_2$ dimer this seems to be mainly enthalpy-driven process. On the other hand, the newly constructed NPII$_2$ dimer, received by simply removing the ligand molecules from their binding sites, needs as many as 20 ps of the dynamics, see Fig. 3, to achieve reasonably stabilized fluctuations in time.

The evolution of NPII$_2$/dipeptide$_2$ and NPII$_2$ geometries is shown in the respective contour plots in Figs. 4 and 5. The initial changes in energy (Figs. 2 and 3) do not seem to correlate with the geometrical changes since the latter are either local fluctuations or local drifts, systematically evolving in the 40 ps timescale. Since the second halves of the trajectories look for both the free and the ligand-carrying dimer equilibrated good enough in terms of energy and geometry as well, the fluctuations representing the last 20 ps have been averaged out to give time-averaged structures for both free and associating dimers. The C$^{\alpha}$-traces of the latter were compared among themselves. In addition, the averaged associate was compared with its starting structure (whose C$^{\alpha}$-trace was identical with the PDB source). In those comparisons, the first seven *N*-terminal residues were disregarded

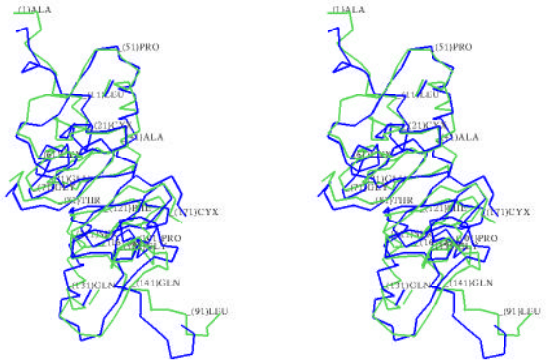

Figure 6. *Overlap (C^{α}-trace) of the NPII$_2$/dipeptide$_2$ complex in the solid-state [5] (blue) with that averaged over the last 20 ps of the molecular dynamics in water (green). RMS=2.52 Å for the C^{α} atoms, with residues 1-7 disregarded.*

as ones having flexible structure, in accord with the original work [5,6] and the relevant PDB source.

A similar dynamics performed for a monomer has demonstrated a considerable deformation of the starting structure, terminated with a relative stabilization of the drifts during the final 10 ps (not shown). A structure averaged out over that time period demonstrated the root-mean-square (RMS) deviation equal to 3.49 Å, with a maximum deviation (Gln^{58}) approaching 8.18 Å. The results clearly demonstrate that NPs cannot function as monomers, in accordance with the experimental findings [6].

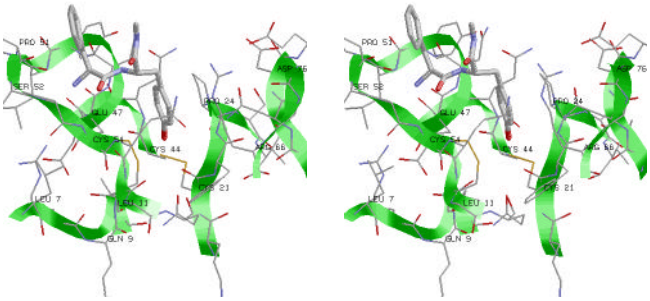

Figure 7. *The hormone binding site with the dipeptide bound to it. This is an enlarged fragment of the structure averaged from molecular dynamics (green in Figs. 6 and 8). It is so aligned as to comply as much as possible with the view in Fig. 4, Ref. [5].*

Comparison of the time-averaged NPII$_2$/dipeptide$_2$ with its PDB source.

The time-averaged structure of the complexing dimer compares to its PDB source with the RMS = 2.52 Å (α-trace, residues 1-7 disregarded). In the both monomers, the largest drifts (up to ca 5 Å) are observed in the reverse loops (residues GPGG, 14-17) connecting the first and the second β-strand in the first domains. In addition, a similar drift is observed in a corresponding loop in the second domain of the second monomer (residues PCGSG, 60-64), see Figs. 1a, 4 and 6. Also, in the first monomer, a deviation within the inter-domain connecting chain (residues SG, 56-57) results from the dynamics, see Figs. 4 and 6. The most preserved (and, incidentally, most buried) regions of the NPII$_2$/dipeptide$_2$ structures belong to the inter-monomer interface. This interface is accomplished by symmetrical interactions involving the first and the second domains of both monomers. Each pair associates antiparallelly by means of the respective 4-th ß-strands, made of LGCFVG, 32-37, in the first and of SCVTE, 78-82, in the second domains, Fig. 6. The results obtained confirm a greater flexibility of the inter-domain connecting chain and of the exposed regions around the first and the second β-strands in both neurophysin domains.

Ligand binding mode.

Despite some apparent differences between the shapes of the solid-state [5] and the time-averaged structures in water (e.g. see Fig. 6), the ligand binding mode in the latter, resulting from the dynamics in solution, is very similar to that in the solid state, see Fig. 7 vs Fig. 4 in Ref. [5]. In particular, all significant polar interactions (ligand's NH_3^+ versus C=O of E47, L50, S52 and versus γ-COO^-E47/R8 salt bridge), as well as nonpolar ones (ligand's Tyr ring versus the C10-C54 and C21-C44 disulphide bridges, CFGP, 21-24, backbone and P24, E47 and N48 side chains) [5], have been retained, see Fig. 7. This confirms that the mode of the protein-ligand interaction is the same in the solid state and in solution.

The finding is of particular value in view of the recent comparative NMR work in solution by Breslow *et al.*, who convincingly argue [12] that the side chains of the ligand's Tyr^2 have similar conformations (*viz. gauche*$^-$-like ones, χ_1 -60°) in the bound dipeptides as in the bound OT, both in solution and in the solid state. This is in contrast with a former conclusions by Lippens *at al. [13]* who, using transfer NOE measurements for the NPI/OT complex, postulated for Tyr^2 residue χ_1 +90°, i.e. a disturbed *gauche*$^+$-like state. Breslow *et al.* base their arguments on (i) the similarities in the chemical shift changes of the ring protons in Tyr^2 that accompany the transfer of a ligand from a free to the bound state [12]. Simultaneously, they (ii) prove the assignments made in a former work by Lippens *at al.* [13] to the ring protons of NPI Phe^{22} to be wrong, as actually belonging to the free (not associated) ligand's Tyr^2 protons. Thus, the 2D NMR cross-

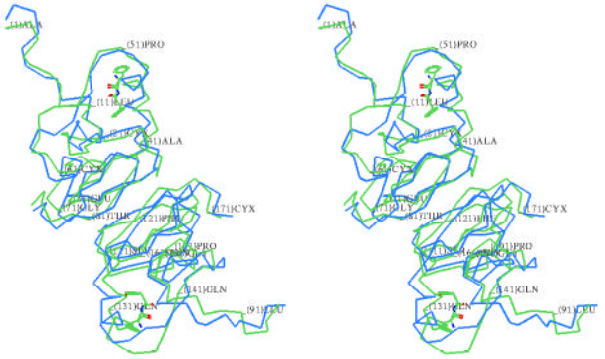

Figure 8. *Overlap (C^{α}-trace) of the $NPII_2$/$dipeptide_2$ complex, averaged over the last 20 ps of the dynamics, (green) with similarly averaged free NPII dimer (blue). RMS=2.20 Å for the C^{α} atoms, with residues 1-7 disregarded. A looser binding between the second domains (in front) at the monomer-monomer interface in the free dimer, as compared to the $NPII_2$/$dipeptide_2$ complex, is clearly seen. This is reflected in the decrease of the respective interaction energy term by ca 12 kcal·mol^{-1}.*

peaks taken in Ref. 13 as those arising from the Tyr^2(ligand)-Phe^{22}(NPI) NOE are proven to be actually due to a Tyr^2(bound) Tyr^2(free) exchange [12]. Our current findings (Tyr^2 side chain in a *gauche*$^-$-like form, see Fig. 7) being in complete agreement with these results, prove that the modeling strategy employed is reliable and efficient. Moreover, common bound conformations for the peptide backbone involving ligand's residues 1 and 2, and the side chains of the key residue Tyr^2 in the dipeptide and OT, both in the solid state and solution [12], provides us with a convenient template for anchoring hormones in the binding sites by simple replacements of the dipeptide with the corresponding fragments of OT or VP in the NPI and NPII binding sites, respectively.

Comparison of the free and complexing dimer

The time-averaged structures of the free and complexing dimer compare mutually with RSM = 2.20 Å (C^{α}-trace). All three-dimensional structural features, typical of the solid-state geometry of NPII [5] have been preserved in the both time-averaged structures, i.e. in NP_2/$dipeptide_2$ and in NP_2. In the first monomers, the largest local differences between NP_2/$dipeptide_2$ and NP_2 are observed in the residues SG, 56-57. These residues make a part of the inter-domain connecting chain, just past the ligand binding loop (ENYLPSPC, 47-54). This loop accommodates the *C*-terminal end of the 3_{10} helix (AEALRCQEENY, 39-49) and the beginning of the inter-domain connection (LPSPCQSGQ, 50-58) just mentioned. In the second monomer, the largest local differences between NP_2/$dipeptide_2$ and NP_2 are observed close to the apex of the binding loop, S52, and, more profoundly, in the region of the first ß-strand in the second domain (residues QKPCG, 58-62). Both, the inter-domain connection and the first β-strand in each domain (residues 11-13, first domain, and 59-61, second domain) are not only exposed to the solvent but also do not demonstrate a distinct secondary structure either in NP_2/$dipeptide_2$ or in NP_2, Fig. 8. Thus, the differences between the free and the complexing dimer, while quite justified in the ligand binding loop, extend just beyond it onto the reasonably loose inter-domain connection, and also involve the most exposed first β-strand regions in both domains.

Interestingly enough, in the free dimer the second domains stick less tightly to each other than in the associating dimer, see Fig. 8. This is reflected in the respective interaction energy terms that can be extracted from the potential energy values for $NPII_2$/$dipeptide_2$ and $NPII_2$. This term for the former is by ca 12 kcal/mol lower than that for the latter. This is in agreement with the recent conclusions of Breslow *et al*. that the second domains are more flexible than the first ones [12], and with the finding that the ligand binding enhances self-association of NPs [3,4,14]. We speculate that this may be relevant to the allosteric mechanism proposed [3,4] for the association and dimerization. The relatively flexible inter-domain connection, as "feeling" a presence or absence of a ligand could provide, in addition to the 3_{10} helix [12], for a lever supporting the transmission of this feeling to the inter-monomer surface involving the second domains.

Acknowledgement This work was supported by the Polish Scientific Research Committee (KBN), the ICM at the University of Warsaw, and the Informatics Center, MAN Gda´nsk area.

References

1. Land, H.; Schultz, G.; Schmale, H.; Richter, D. *Nature (London)* 1982, *295*, 299-303.
2. Gainer, H.; Russel, J.T.; Loh, Y.P. *Neuroendocrinology* **1985**, *40*, 171-184.
3. Breslow, E.; Burman, S. *Adv. Enzymol.* **1990,** *63*, 1-67.
4. Breslow, E.M.G. in *Vasopressin*, Gross, P.; Richter, D.; Robertson, G.L. Eds.; John Libbey Eurotext, 1993; pp 143-155.
5. Chen, L.; Rose, J.P.; Breslow, E.; Yang, D.; Chang, W.-R.; Furey, Jr., W.F.; Sax, M.; Wang, B.-C. *Proc. Natl. Acad. Sci. USA* **1991**, *88*, 4240-4244.
6. Menendez-Botet, C.; Breslow, E. *Biochemistry* **1975**, *14*, 3825-3835.

7. Bernstein, F.C.; Koetzle, T.F.; Williams, G.J.; Meyer, E.E.J.; Brice, M.D.; Rodgers, J.R.; Kennard, O.; Shimanouchi, T.; Tasumi, M. *J. Mol. Biol.* **1977**, *112*, 535-542.
8. CHEM-X, Chemical Design Ltd. 1994, Chipping Norton, Oxfordshire, OX7 5SR, England.
9. BIOSYM Technologies, Inc. 1992, San Diego, CA, USA.
10. Pearlman, D.A.; Case, D.A.; Caldwell, J.; Singh, U.C.; Weiner, S.J.; Kollman, P.A. AMBER Version 4, University of California, San Francisco, 1990.
11. Jorgensen, W.L.; Chandresekhar, J.; Madura, J.; Impey, R.; Klein, M. *J. Chem. Phys.* **1983**, *79*, 926-935.
12. Breslow, E.; Sardana, V.; Deeb, R.; Barbar, E.; Peyton, D.H. *Biochemistry* **1995**, *34*, 2137-2147.
13. Lippens, G.; Hallenga, K.; Van Belle, D.; Wodak, S.J.; Nirmala, N.R.; Hill, P.; Russel, K.C.; Smith, D.D.; Hruby, V.J. *Biochemistry* **1993**, *32*, 9423-9434.
14. Ruvo, H.; Fassina, G. *Int. J. Peptide Protein Res.* **1995**, *45*, 356-365.